Science Advances
AAAS

Supplementary Materials for

Coral Sr/Ca-SST reconstruction from Fiji extending to ~1370 CE reveals insights into the Interdecadal Pacific Oscillation

Juan P. D'Olivo *et al.*

Corresponding author: Juan P. D'Olivo, dolivo@cmarl.unam.mx

Sci. Adv. **10**, eado5107 (2024)
DOI: 10.1126/sciadv.ado5107

This PDF file includes:

Supplementary Text

Potential sampling artifacts

Coral microstructures have been reported to exhibit a variable geochemical composition, which can impact environmental reconstructions when sampling results in a mixed representation of these structures (*35-37*). To mitigate these issues, various strategies are typically employed. For corals with small corallites, sampling of entire or multiple corallites is recommended, while for corals with large corallites, such as *Diploastrea heliopora*, sampling targets specific skeletal structures (*35-37*), as outlined in the main text.

To minimize these concerns, coral samples targeting the columella were collected at millimeter resolution, with only small volumes of powder (approximately 3 mg) were extracted to ensure shallow sampling tracks, thereby reducing the likelihood of sampling into different structures. Additionally, transects were adjusted to target only sections with clearly exposed corallites. The relatively large size of *Diploastrea heliopora* corallites (approximately 1 cm across) facilitates the selection and targeting of specific structures for sampling.

The slow growth rates (~ 3.7 mm/year) suggest the coral did not experience drastic changes in temperature due to changes in depth as the colony grew up to 3 m below the surface when the core was collected. The change in depth of ~ 3 m experience over > 600 years by this *Diploastrea heliopora* coral compares to expected changes of nearly 6 m for massive *Porites* corals, the most commonly used species for paleo-reconstructions in the Indo-Pacific region, based on typical growth rates of 1 to 2 cm per year (*64*). A progressive change in corallite orientation is observed in the X-rays from near vertical on the top of the colony to ~ 45° in the bottom part of the record. The slow growth rates also indicate the colony was small when the change in growth direction took place (e.g., ~ 40 cm, in its first 100 years), which added to its isolated location, suggest that light regimes were likely not significantly different on top and side of the colony when the coral was sampled at an angle. The similar growth rates at the top and bottom of the colony (3.63 ± 1.06 (1SD; n = 100) mm/year and 3.75 ± 0.98 (1SD; n = 100) mm/y; respectively) support a negligible light effect. In this sense, on a relatively small *Porites* coral, no change in Sr/Ca was observed along completely different sample angles (90°)(*65*). However, when a change in direction appears to affect Sr/Ca, different coral species have consistently been reported to increase their Sr/Ca values (*66, 67*), which would bias reconstructions towards colder values. We observed an opposite behaviour as the section of coral sampled at ~ 45° coincided with lower Sr/Ca (warm values). Furthermore, Sr/Ca and growth rates showed no relationship; together this provides strong evidence for no clear growth rate effects.

Another potential source for spurious temperature reconstructions is the formation of aragonitic or calcitic secondary cements. The XRD data suggested no calcite presence (Fig. S15), and while no data for secondary aragonite is available, this is reported to consistently bias Sr/Ca values towards colder values amongst different coral species reported (*68-73*). A visual inspection of the core under a microscope indicated no apparent alteration but even 2.5 to 3% secondary aragonite would result in 0.5 to 1.6 ± colder temperatures (*68*). Therefore, any growth or secondary aragonite would mean that the temperature values for the older part of the skeleton (1300s-1400s) should be even higher if affected by secondary aragonite or growth, which is not supported by any other record or reconstruction available (e.g., Fig. 2).

Vital effects on Sr/Ca reconstructions

Environmental reconstructions from coral and other bio-geochemical proxies, including Sr/Ca, can be affected by the so called “vital effects” (*74*), a term used to group all physiological processes that can affect proxy incorporation and their interpretation. Despite these potential

issues when vital effects remain relatively constant Sr/Ca can produce excellent reconstructions as attested by a large of bibliographical evidence showing how well the proxy typically works.

To minimize the effects from vital effects, we followed suggestions by the PAGES coral community to use composite Sr/Ca records to cancel out local noise in individual Sr/Ca records (*75*). We also took several precautions during the sampling, as detailed in the previous section. The congruence between our 627-year record and a multi-proxy reconstruction (PHYDA, PAGES Ocean 2K) is notably compelling. Additionally, Kanathea is a small, virtually uninhabited, island spanning 2 km in near oceanic conditions, further diminishing the influence of local factors, making it ideal for paleoceanographic reconstructions, although local reef circulation issues. Nevertheless, future work should focus in expanding the range of proxies studied, advocating for a multiproxy approach (*76*) encompassing other temperature proxies like Li/Mg and Sr-U (*77, 78*).

Climate models

CESM version 1.1 (CESM1-CAM5) was developed at the National Centre for Atmospheric Research (NCAR). The atmosphere model component is the Community Atmosphere Model version 5 with a horizontal resolution of approximately 2° latitude x 2° longitude, and the ocean model component is the Parallel Ocean Program version 2 with a horizontal resolution of approximately 1° latitude x 1° longitude. Otto-Bliesner, Brady, Fasullo, Jahn, Landrum, Stevenson, Rosenbloom, Mai and Strand (*53*) provide more details of the CESM Last Millenium Ensemble. We also extract the SWCP gradient from Last Millennium simulations using CMIP5 models MPI-ESM (*54*) and CCSM4 (*55*) (Fig. S6). The Max Plank Institute Earth System Model (MPI-ESM)(*54*) paleo configuration is used for the Last Millennium simulations with an ECHAM6 atmosphere component at approximately 2° horizontal resolution and an MPIOM ocean component at approximately 1.5° horizontal resolution. The Community Climate System Model version 4 (CCSM4)(*55*) is a predecessor of CESM and is comprised of the Community Atmosphere Model version 4 and the Parallel Ocean Program version 2, both run with horizontal resolutions of approximately 1° in the Last Millennium simulation.

The external forcings that drive palaeoclimate simulations including the CESM LME and the Last Millennium simulations from MPI-ESM and CCSM4 are estimations of the real external forcings, derived chiefly from polar-ice core data. The greenhouse trace gases were derived from concentrations in air bubbles trapped in the ice-cores. Volcanic activity is derived from the acidity of the ice layers in polar-ice cores, interpreted with simple models that consider the simultaneous appearance of pH spikes in Greenland and/or Antarctica ice cores to estimate the intensity and location of past eruptions. Past solar activity is derived from the concentration of the cosmogenic isotope ^{10}Be in ice cores. This isotope is produced in the stratosphere by cosmic rays, which are deflected by the solar and terrestrial magnetic field, and then deposited on the surface with precipitation. After subtracting the effect of the Earth's magnetic field, the cosmogenic isotope concentrations are interpreted as a measure of solar magnetic field and, indirectly, of the solar output. Land-use forcing changes are reconstructed from estimates of historical population density and agricultural intensity. This forcing is, however, considered generally weaker than the other paleo forcings. The time resolution of the volcanic and greenhouse forcing is annual for most of the past millennium, with dating uncertainties of ±1 year for some volcanic eruptions. The temporal resolution of the solar forcing is somewhat coarser at approximately decadal scale.

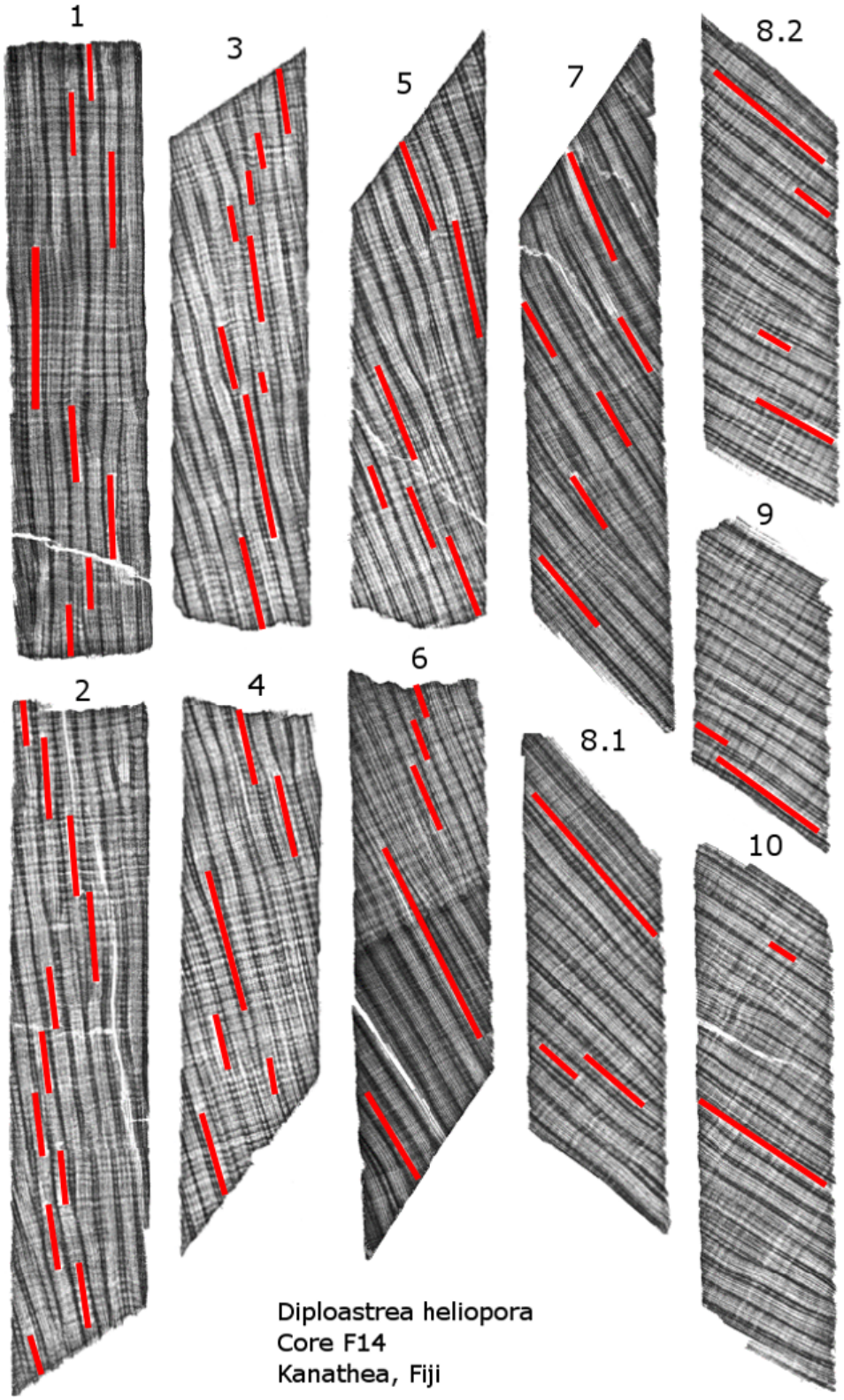

Fig. S1. X-radiograph positive for core F14. Coral slabs are shown from core top to bottom (1 to 10). Annual bands (~0.4 cm), perpendicular to the large corallites (0.8 to 1 cm wide). Red lines used to highlight the sampling transects along the main growth axis. The frequent change in transect was necessary to ensure that only columella material was sampled.

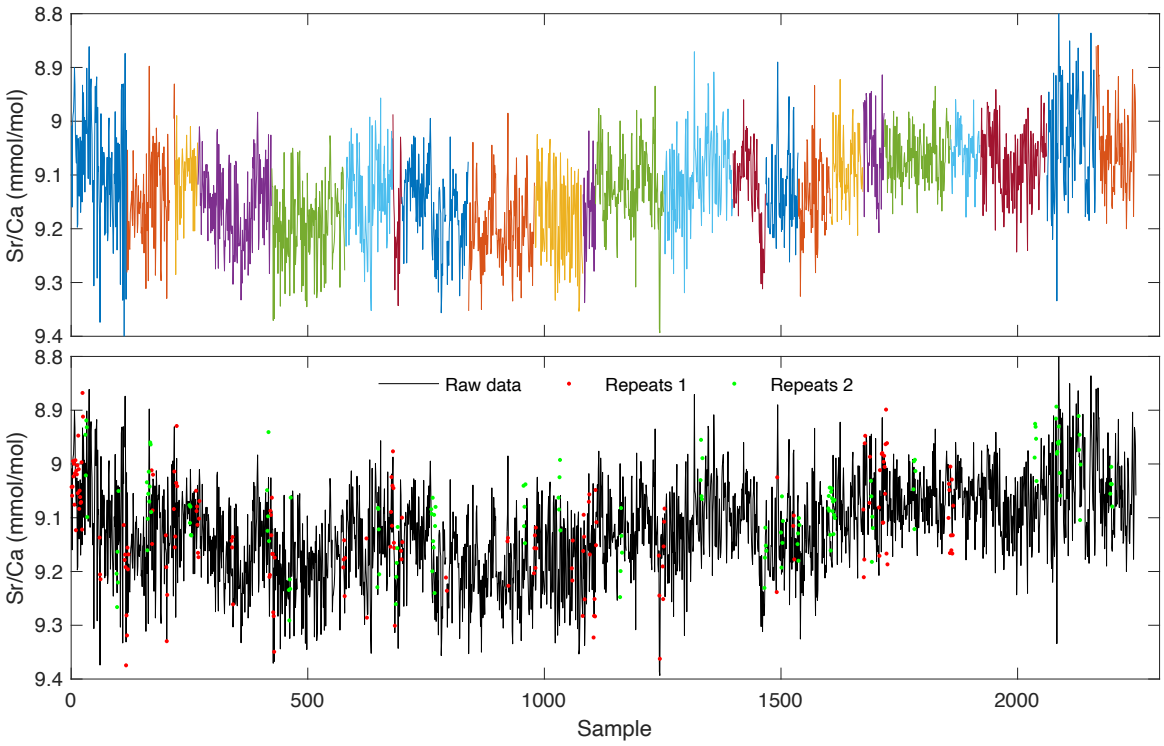

Fig. S2. Raw coral Sr/Ca data. Subannual (2 to 7 samples per year) record of coral Sr/Ca for Fiji core F14. The top panel shows the Sr/Ca data separated by analytical tracks to show the connection between sections, the bottom panel shows the Sr/Ca as a continuous record (black) and the repeats (colored dots). The repeats correspond to separate sample aliquots divided in two analytically sessions (red and green).

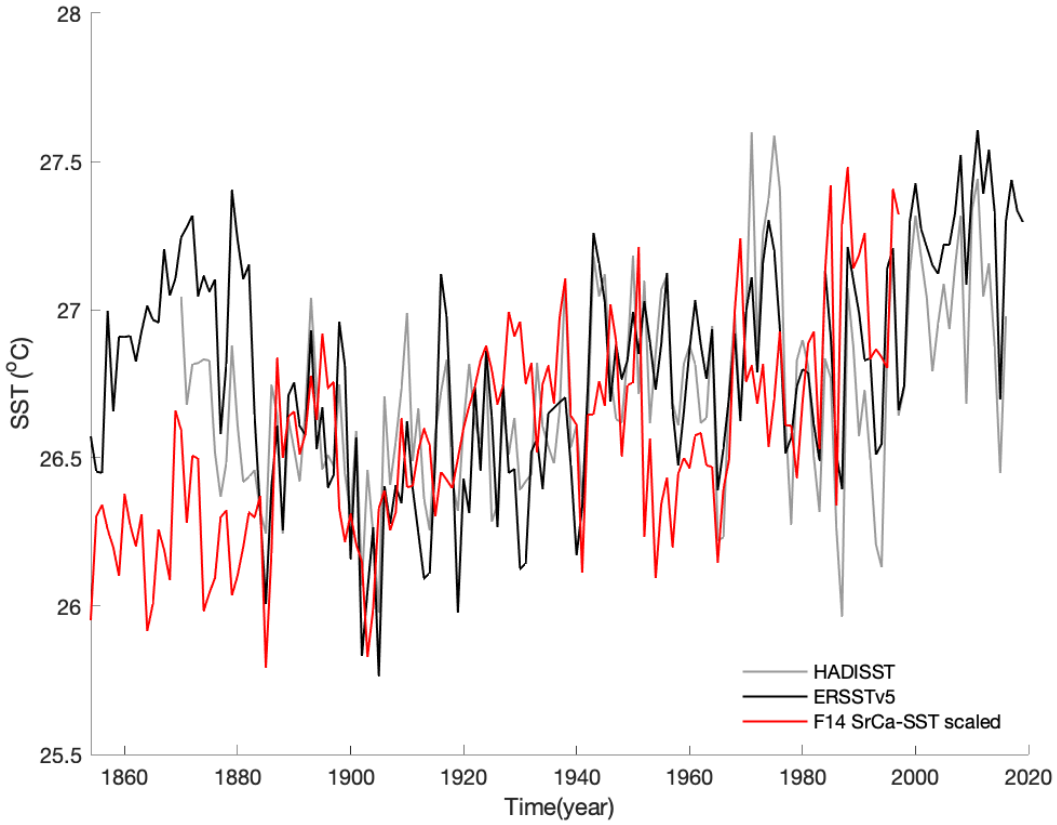

Fig. S3. Comparison of coral SST with instrumental SST. "Best" SST reconstruction based on scaled Sr/Ca coral data from core F14 (red) compared against instrumental records from ERSSTv5 (black) and HADISSTv1 (grey) centered around 18 °S and 180 °W.

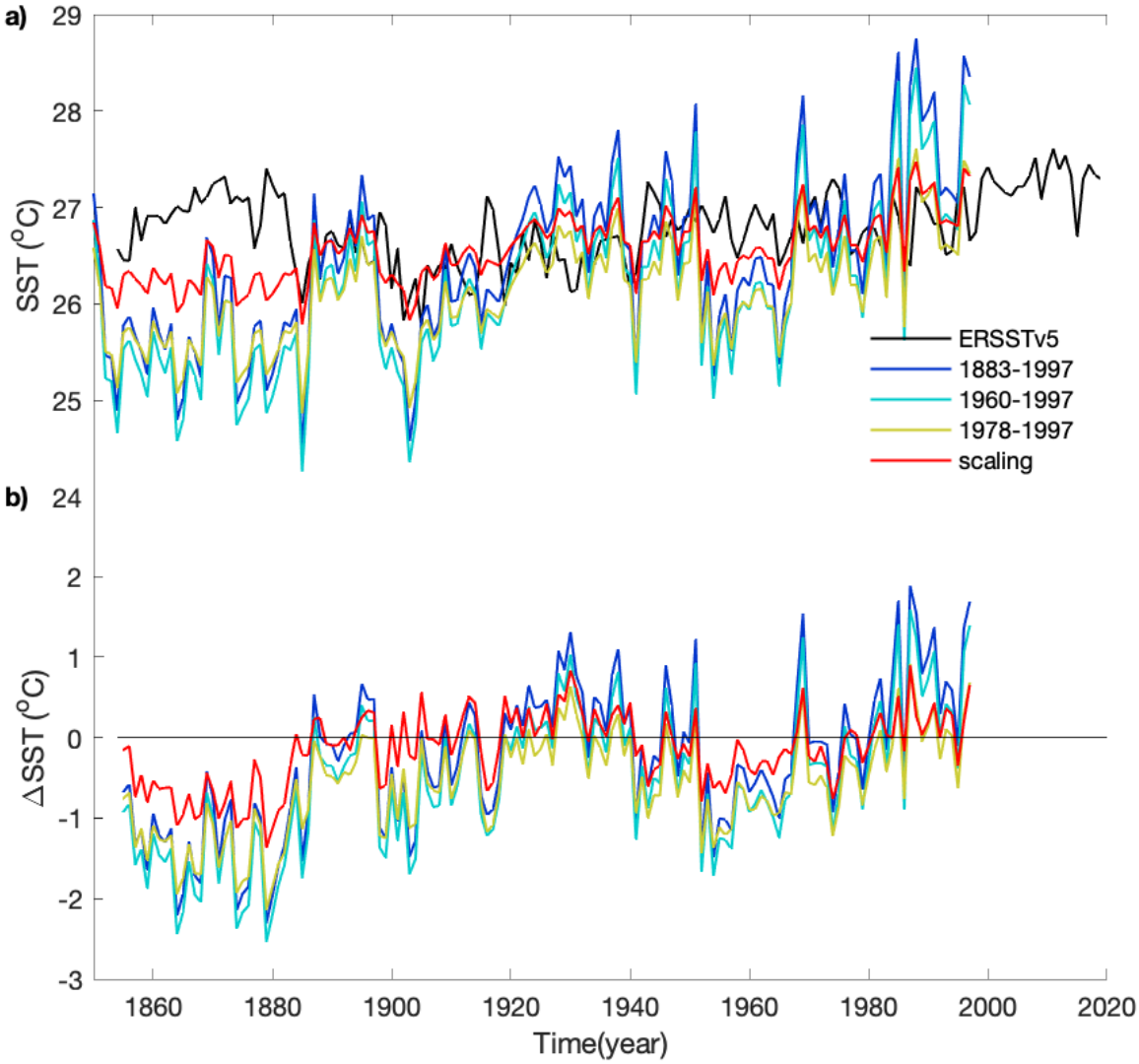

Fig. S4. Comparison of different SST calibrations applied to core F14. a) SST reconstructions from the Fiji coral Sr/Ca data obtained for different calibration periods and the scaling approach described in the methods section. b) residuals between the Fiji SST-Sr/Ca derived data and the instrumental SST data from ERSSTv5 for the grid point closest to Fiji (18 °S 180 °W).

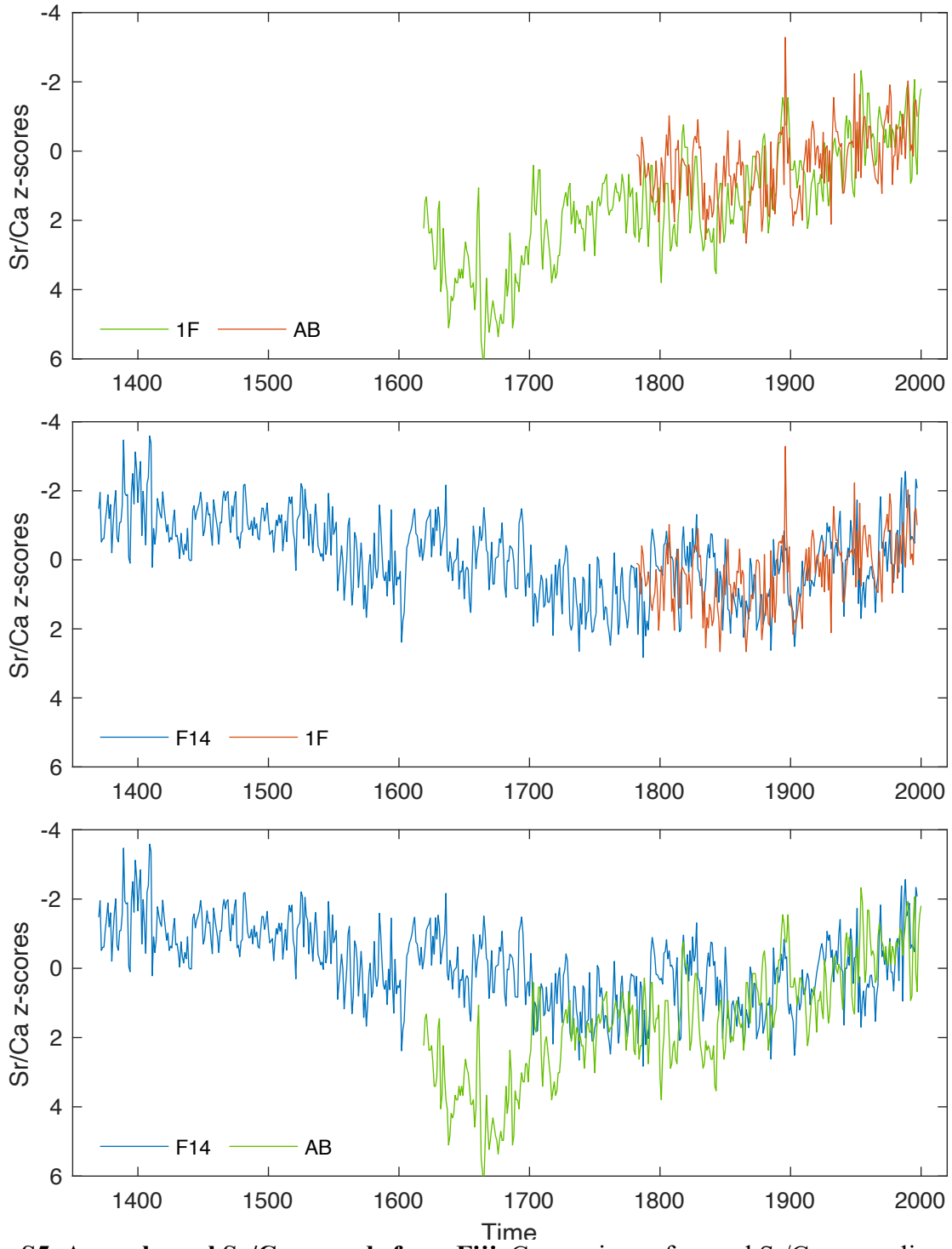

Fig. S5. Annual coral Sr/Ca records from Fiji. Comparison of annual Sr/Ca anomalies reconstructed from core F14 (blue) with a) the Sr/Ca anomalies of the Porites corals 1F (green) and AB (orange) from Fiji (*23*). Anomalies were calculated for the annual data relative to the mean and standard deviation for the 1883 to 1997 period. Only the data covering the overlapping period (1781-1997) from core AB was used in the calculations of the Fiji composite calculations as the early parts of the records show anomalous values and there are much higher age and analytical uncertainties for this record (Brad Linsley, personal communication).

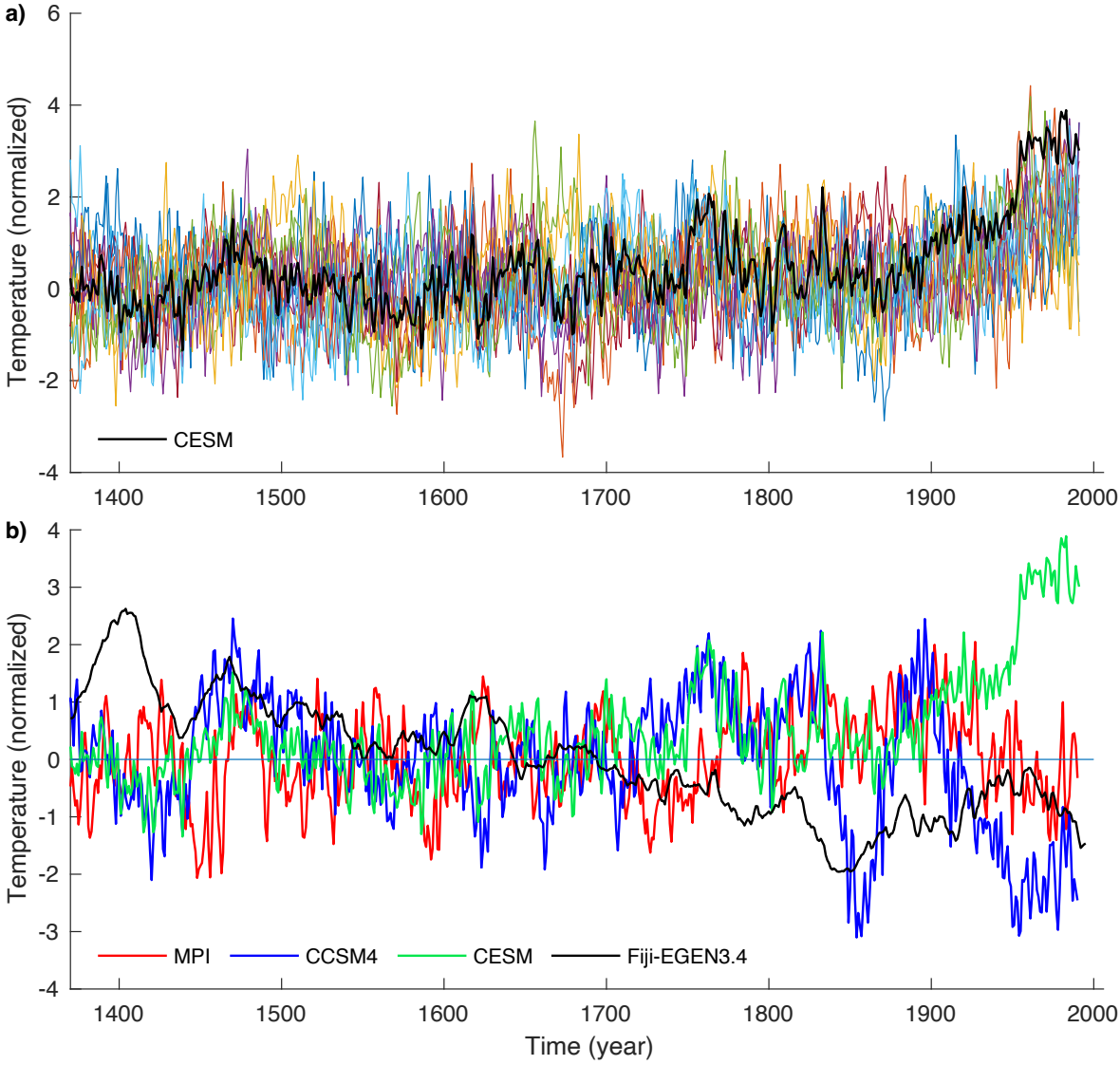

Fig. S6. Climate simulations of the Pacific SWCP SST gradient. (a) Thirteen simulations from the CESM LME (*53*) (coloured) and their average (black). (b) Climate simulations of the SWCP from MPI-ESM-P (*54*) (red), CCSM4 (*55*) (blue) and the ensemble-average from CESM (green, same as black line in panel (a)) compared to the calculations based on the Fiji composite data and the EG-N3.4 data. A 31-yr running average was applied to all the data.

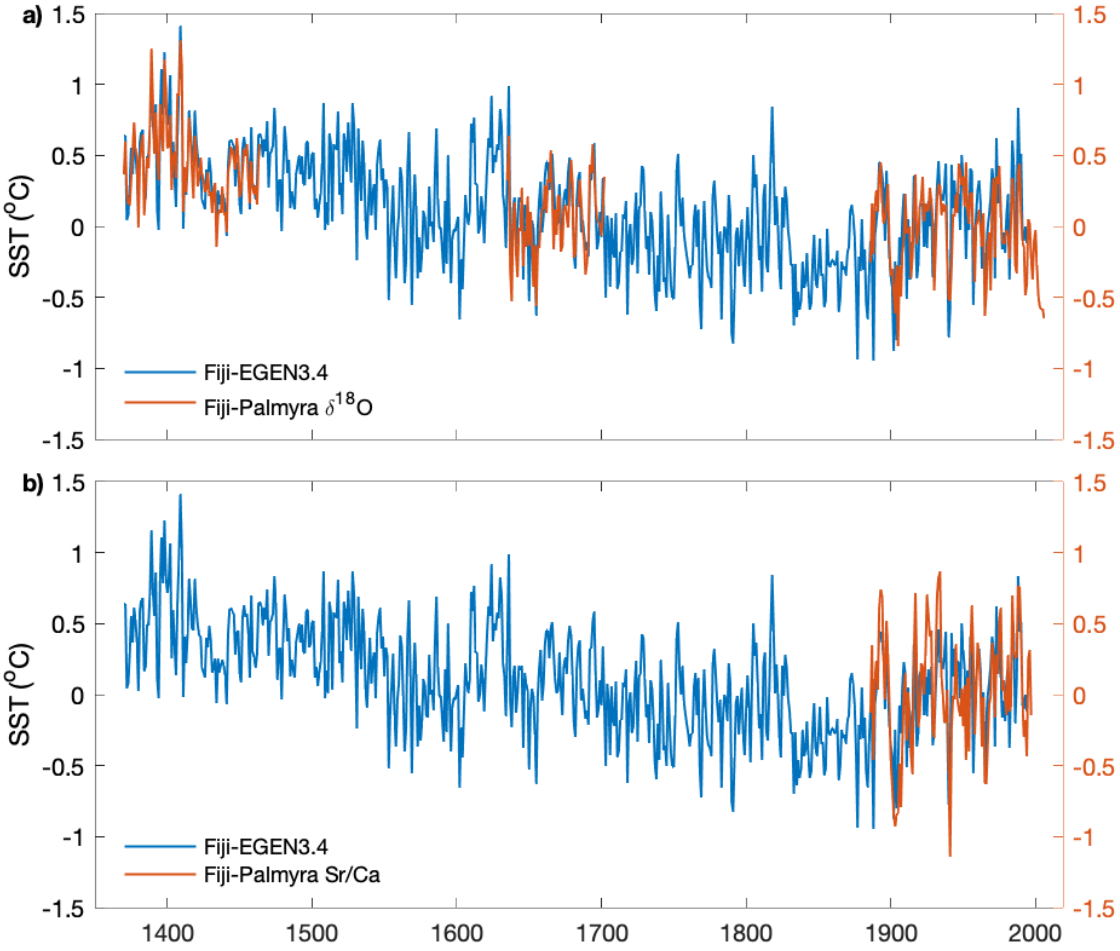

Fig. S7. Comparison between southwestern and central Pacific SST gradient reconstructions. The composite Sr/Ca Fiji-Niño3.4 SST SWCP gradient (Fiji-EG-N3.4; blue) compared to: a) the gradient based on the SST difference between Fiji composite Sr/Ca-SST and Palmyra coral δ^{18}O-SST (*60, 79, 80*), and b) the gradient based on the SST difference between Fiji composite Sr/Ca-SST and Palmyra coral Sr/Ca-SST (*58*). Anomalies were computed relative to the 1961 to 1990 reference period.

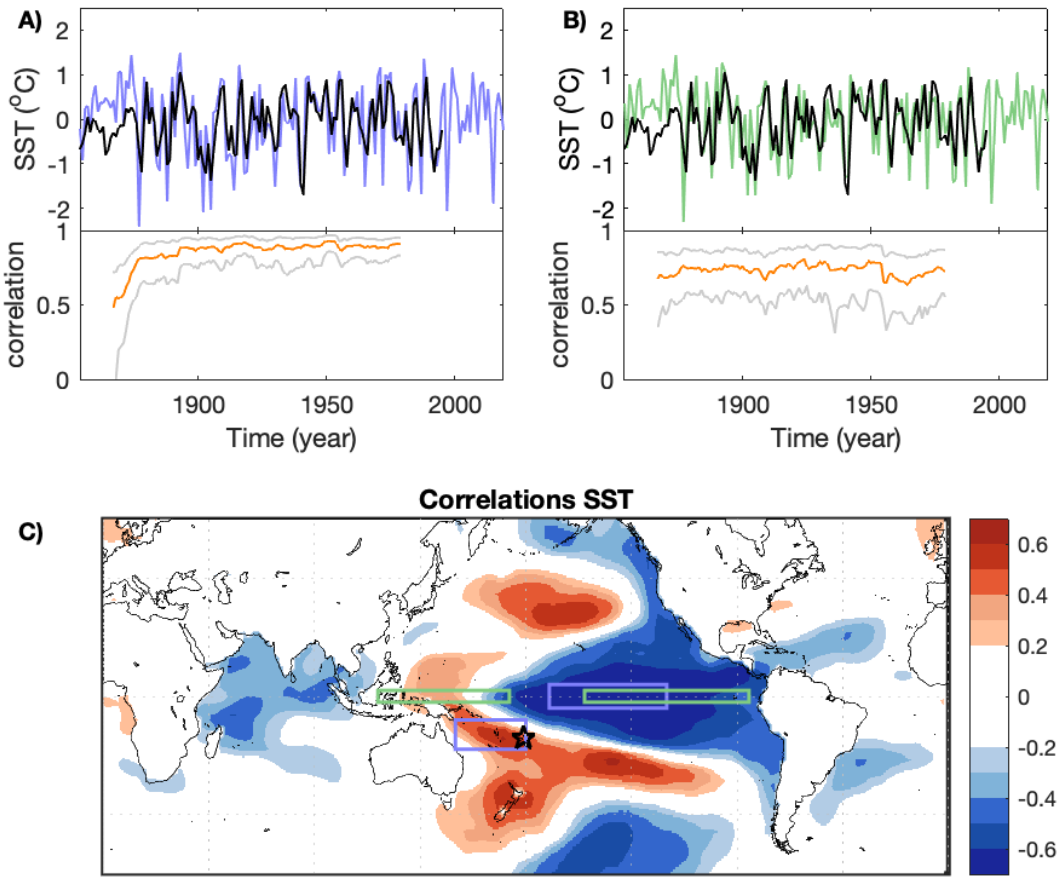

Fig. S8. Comparison between reconstructed and observational SST Pacific gradients. Comparison between average reconstructed SWCP (black line) with: A) the instrumental ERSSTv5 SST SWCP gradient as defined in Fig. 1C (purple line) and B) the zonal gradient (*57*) (green line). In each case the running correlation for a 31-year window is shown between the coral and instrumental reconstructions (orange line) and their 95% confidence intervals (grey line). C) Spatial correlations between the reconstructed SWCP and mean annual ERSSTv5 SST. Highlighted in C) are the areas defining the southwestern-central (purple areas; SWCP) and zonal gradient (green areas), and the location of Fiji (black star) used to reconstruct the SST gradients in panels A and B.

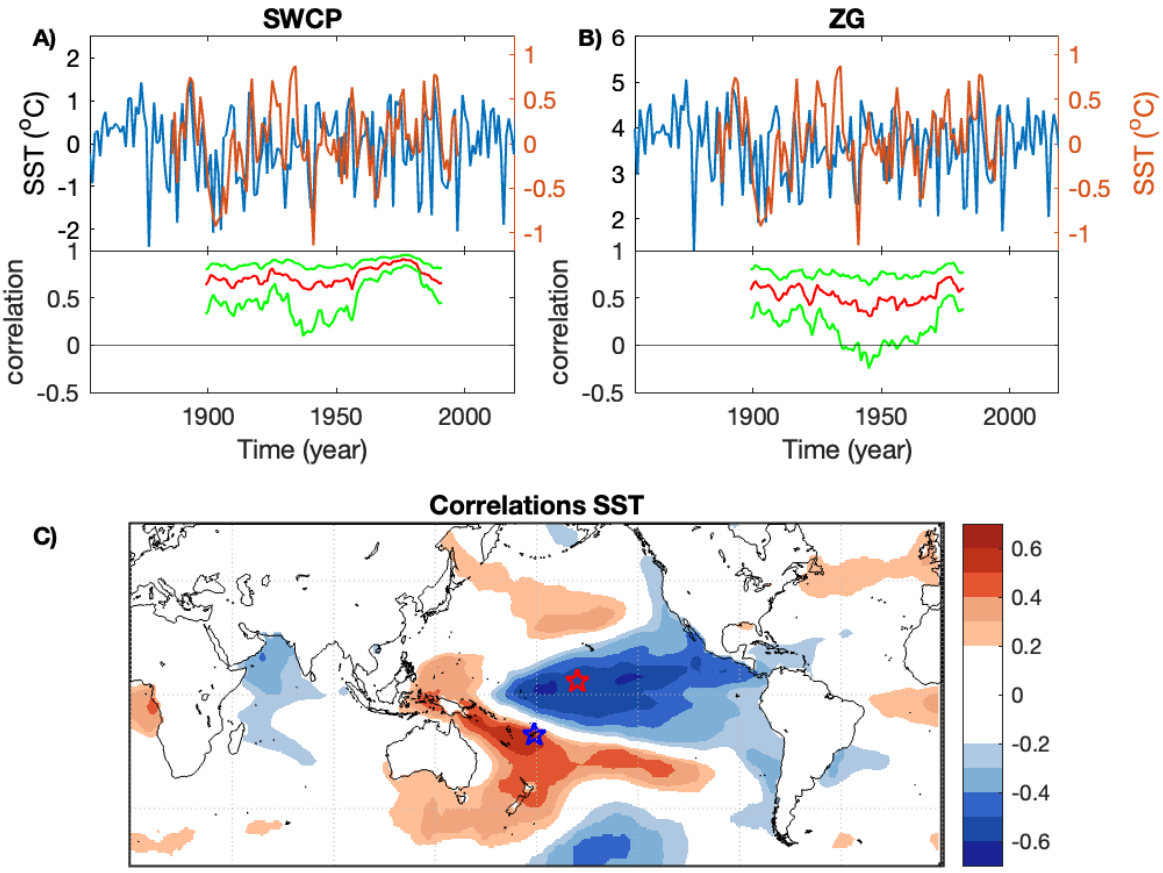

Fig. S9. Validation of the SWCP gradient with coral data from Palmyra. Southwestern-central Pacific SST gradient based on the SST difference between Fiji and Palmyra coral Sr/Ca-SST (Fig S7B) compared with A) the SWCP based on instrumental data and B) the zonal SST gradient as defined in (*57*) based on instrumental data from ERSSTv5 SST. 31-year running correlations in a and b shown below with green lines indicating the 95% confidence interval for the correlations (red lines). C) Spatial correlation of SWCP based on the SST difference between Fiji and Palmyra coral Sr/Ca-SST with ERSSTv5. Highlighted is the location of Fiji (blue star) used to reconstruct the SST gradients and Palmyra (Red star) used to calculate the SWCP in Panels A and B.

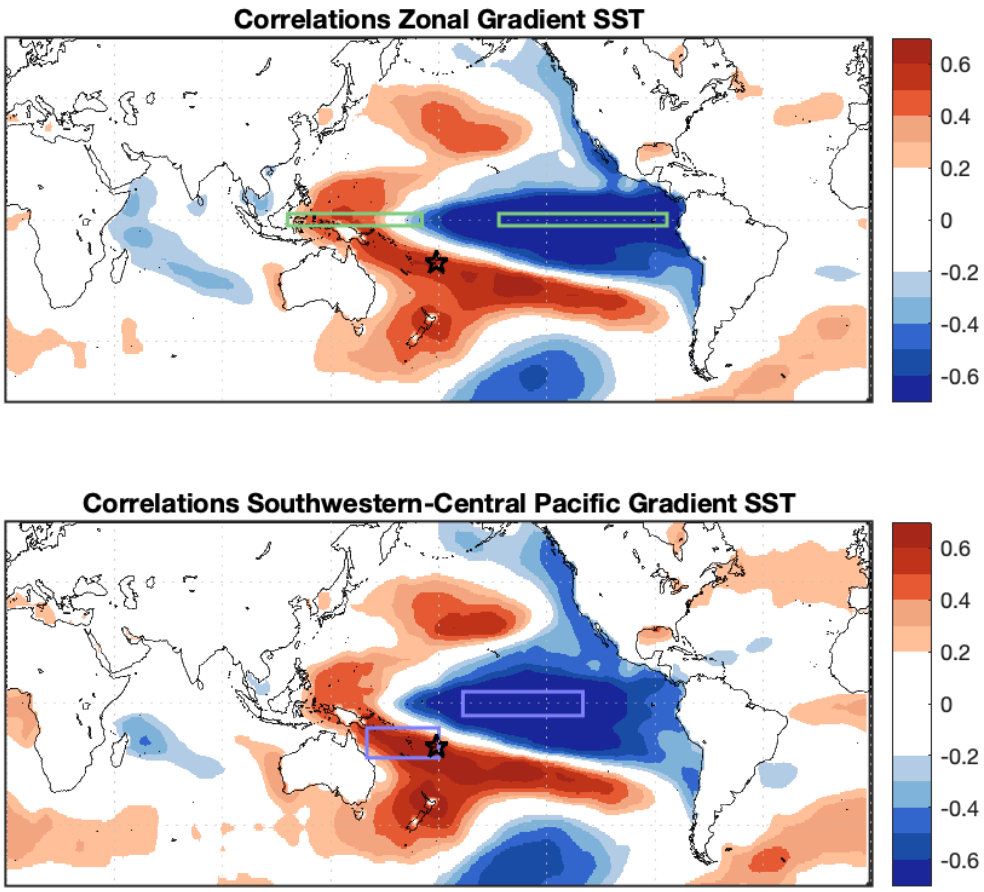

Fig. S10. Relationships between the zonal and southwestern-central Pacific gradient with SST. Spatial correlation for the Zonal SST gradient (zonal gradient)(*57*) (Top) and the southwestern-central Pacific SST gradient (SST) (Bottom) based on the SST from ERSSTv5 data for July-June annual averages. Highlighted are the areas defining the southwestern-central (purple areas; SWCP) and zonal gradient (green areas), and the location of Fiji (black star) used to reconstruct the corresponding SST gradients.

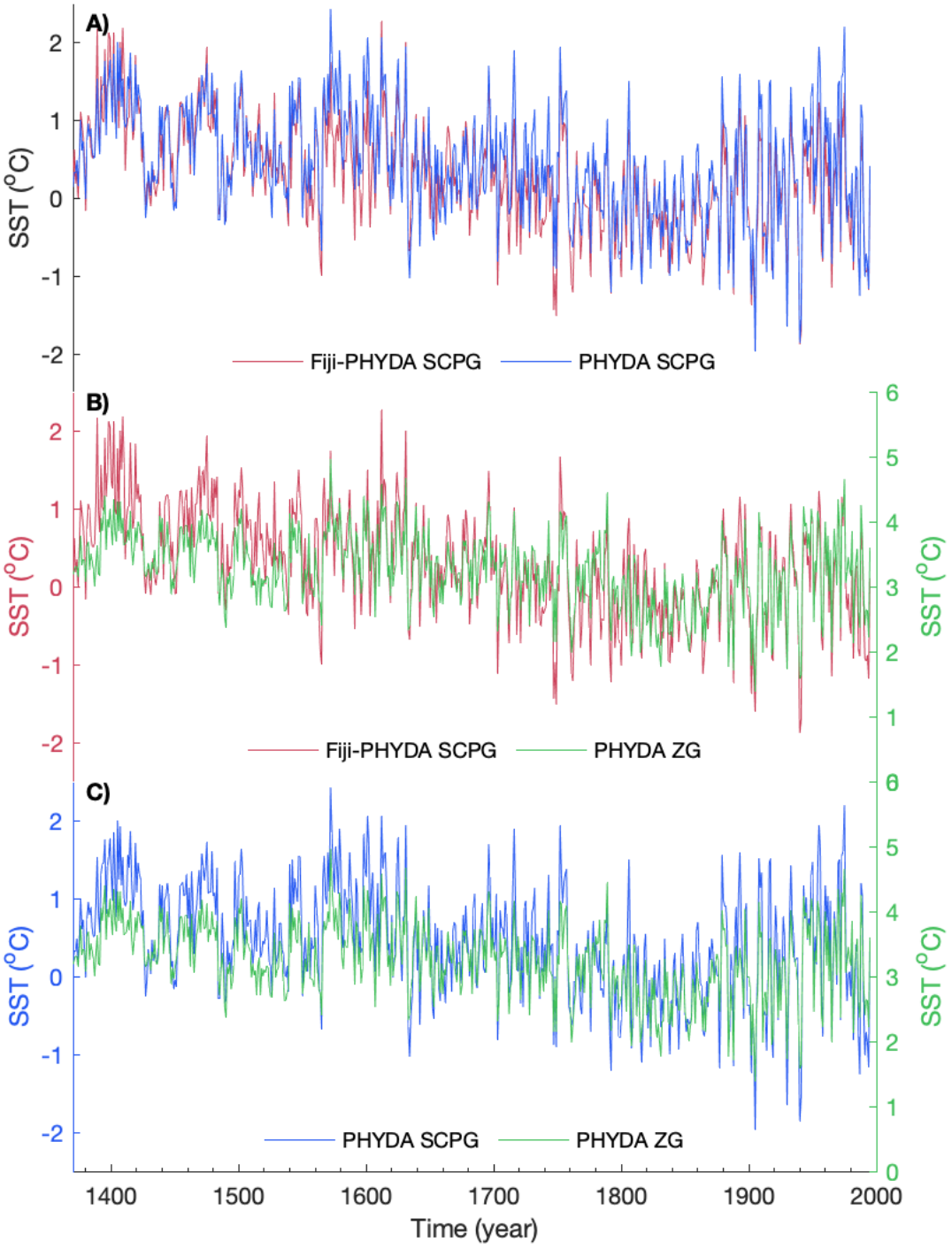

Fig. S11. Comparison of SST gradients in the Pacific. A) Annual records for the southwestern central Pacific SST gradient (SWCP) calculated as the difference between Fiji composite and PHYDA (*21*) Niño 3.4 compared against the southwestern central Pacific SST gradient as the difference between PHYDA data for the southwestern Pacific and the Niño 3.4 region. B) Annual records for the SWCP calculated as the difference between Fiji composite and PHYDA Niño 3.4 compared against the zonal SST gradient as defined in (*57*) calculated from PHYDA data (*21*). C) Annual records comparing the zonal and southwestern-central Pacific gradients calculated from the PHYDA data only.

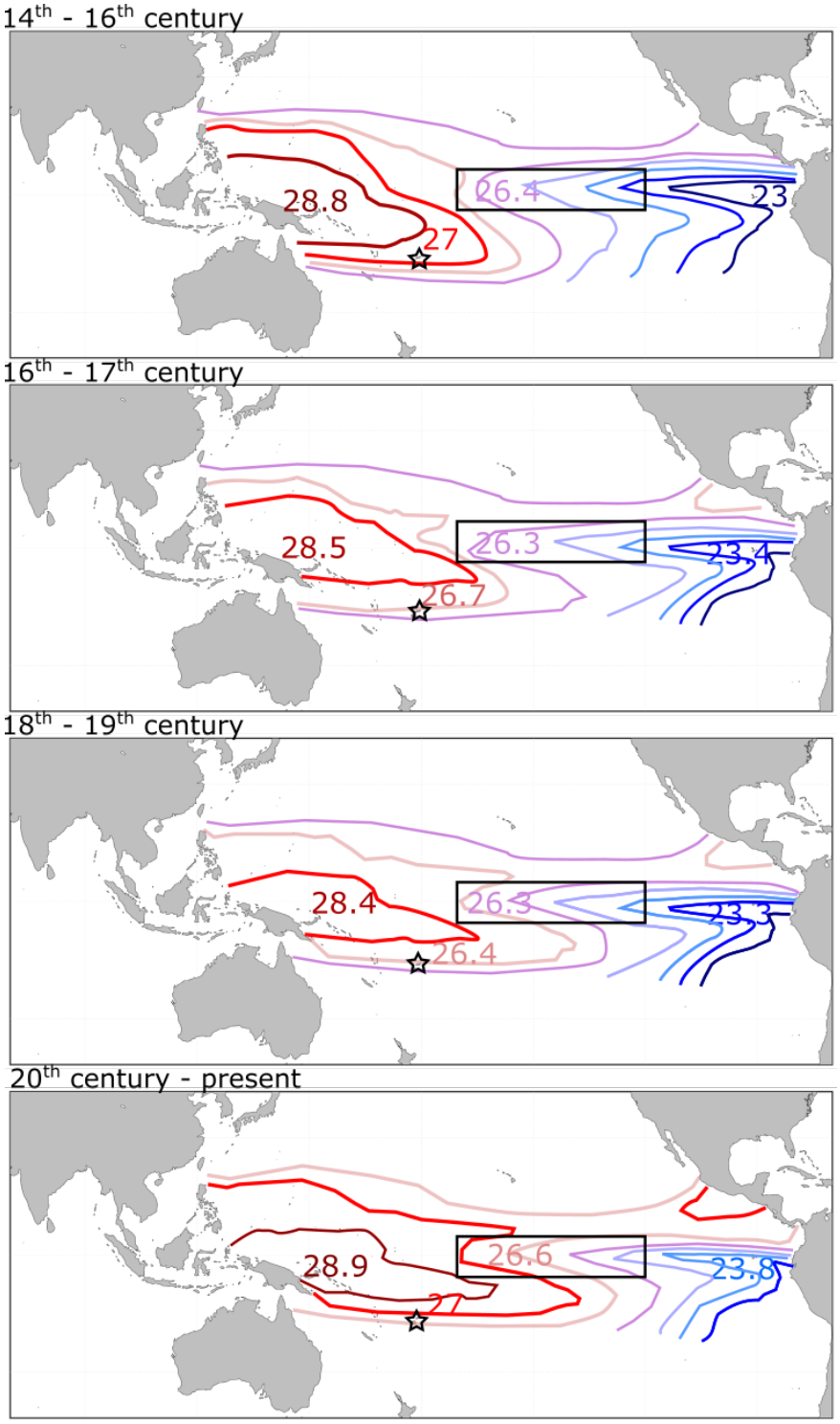

Fig S12. Temperature changes in the tropical Pacific since 1370. Conceptual schematic of the changes in SST in across the tropical Pacific based on reconstructions from Fiji, the Indo-Pacific Warm Pool (*25, 26*), the central Pacific (Nino 3.4 region)(*21, 56*) and the eastern equatorial Pacific (*62*). Each panel represents one of the four periods (1370-1553, 1553-1703, 1703-1920, 1920-1997) identified in the change point analysis from Fig. 1. The values represent the average temperature over the corresponding period for the proxies from the corresponding region. The colour scale is not an absolute but rather highlights relative changes in temperature from one period to another where darker red (blue) colours represent warmer (colder) values and lighter colours milder temperatures.

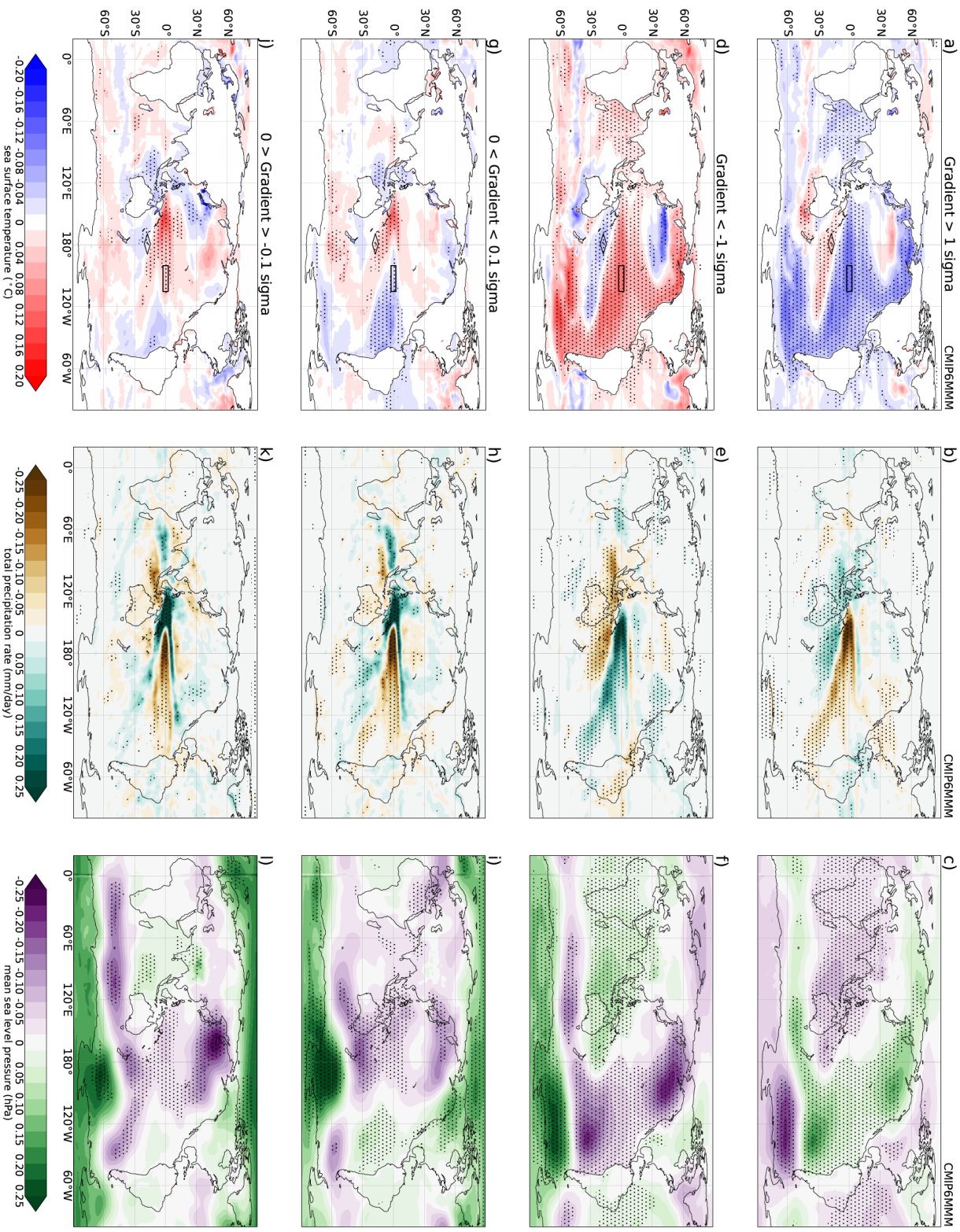

Fig. S13. Composite maps of simulated SST (left column), precipitation (middle column) and mean sea level pressure (right column). In each case four different regimes are included based on the magnitude of the SWCP gradient calculated using data from pre-industrial control simulations of multiple CMIP6 models (16,062 years from 24 CMIP6 models). Panels a-c represent composites obtained when there is a strong positive SWCP gradient (i.e., warmer temperature over Fiji compared to central Pacific and the magnitude of the gradient is stronger

than 1 standard deviation), panels d-f are similar but represent strong inverse SWCP gradient (i.e., warmer temperature in the central Pacific than in Fiji and the SWCP gradient is less than -1 standard deviation). The bottom two rows represent composites when the SWCP gradient is weaker (less than 0.1 standard deviation) with panels g-i showing composite maps when the gradient is weaker and positive and panels j-l represent composites when the gradient is weaker and negative. Stripling on the plots represents significant values at 95% significance level using a two-tailed t-test. Composites from each model are computed first before calculating the multi-model mean composite to provide equal weightage to each CMIP6 model used in the study.

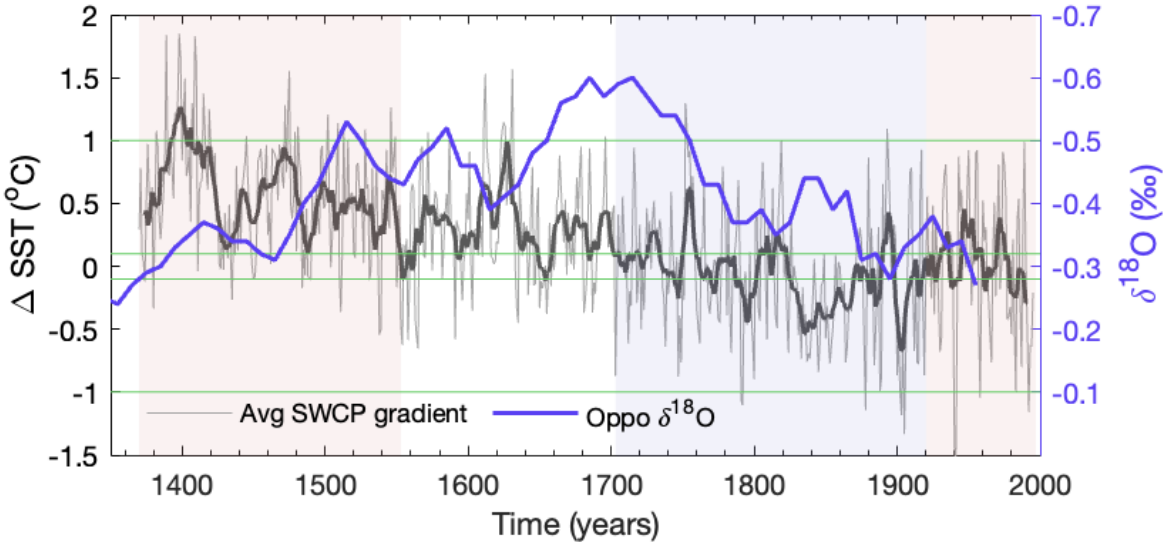

Fig. S14. Comparison between SWCP temperature gradient and the hydrology of the WPWP. Average Annual and 15-year moving average SWCP gradient (black) compared to the hydrology reconstruction for Makassar Strait near Indonesia in the WPWP based on seawater $\delta^{18}O$ from sediment cores (*26*). Warm (cold) periods in the Fiji composite highlighted in red (blue) based on the change point analysis from Fig.1. Also shown are gradient reference values for the average SWCP gradient as used in Fig. 4 (horizontal green lines).

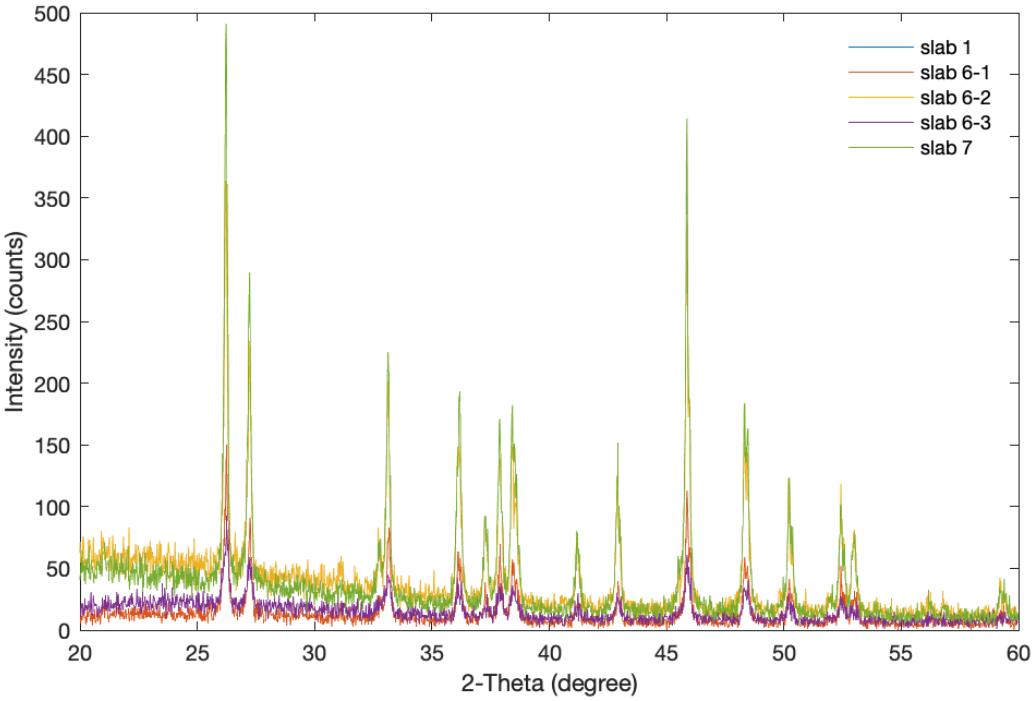

Fig. S15. X-ray powder diffraction pattern. XRD profiles for five coral powder samples from coral core F14 from top middle and bottom slabs displaying the characteristic profile of aragonite. Slabs 1 and 7 were sampled near the middle, while slab six was sampled in three locations (top, middle and bottom).

Table S1. ^{230}Th/U-dating of core F14. Results of ^{230}Th/U-dating of a coral piece collected from section 10 at the bottom of coral core F14. The age is referenced to the year of dating (AD 2023).

Sample	**^{238}U [µg/g] (±)**	**^{232}Th [ng/g] (±)**	**(^{234}U/^{238}U) (±)**	**(^{230}Th/^{238}U) (±)**	**age uncorrected [ka] (±)**	**age corrected [ka] (±)**	**(^{234}U/^{238}U) Initial (±)**
F14 10	2.604 (0.017)	0.03306 (0.00037)	1.14154 (0.00037)	0.006926 (0.000021)	0.6638 (0.0020)	0.6635 (0.0020)	1.14180 (0.00040)

Table S2. Comparison of coral F14 with instrumental and reconstructed SST. Pearson correlation coefficients for F14 Sr/Ca record against instrumental SST records for the area centred closest to the study site and for the regional reconstructions for the Western Pacific region from Tierney, Abram, Anchukaitis, Evans, Giry, Kilbourne, Saenger, Wu and Zinke (*24*) based on instrumental data of HADISST (Target O2K SST; 1871-2006) and coral geochemical records (WP O2K reconstruction; 1617 to 1997). Significance 95% showing in parenthesis. Comparison with OISSTv2 covers the period 1982-1997 due to the shortness of this record.

Period	OISSTv2	ERSSTv5	HADISST	Target O2K SST	WP O2K reconstruction
1978-1997	-0.54 (0.03)	-0.50 (0.04)	-0.37 (0.11)	-0.44 (0.05)	-0.26 (0.29)
1960-1997		-0.30 (0.07)	-0.14 (0.40)	-0.57 (<0.001)	-0.46 (0.004)
1883-1997		-0.39 (<0.001)	-0.25 (0.007)	-0.46 (<0.001)	-0.50 (<0.001)
1718-1997					-0.51 (<0.001)
1617-1997					-0.37 (<0.001)

Table S3. Residuals for SST calculated from core F14 Sr/Ca data. Root mean square mean error (RSME, units °C) in Sr/Ca-SST reconstructions from core F14 based on different calibration periods and the ERSSTv5 instrumental data. In all cases the RSME was calculated for the period 1883-1997.

Calibration period	Fiji F14-Sr/Ca
1883-1997	0.75
1960-1997	0.77
1978-1997	0.63
Scaled 1883-1997	0.36

Table S4. SST change calculated for core F14. Linear temperature trends (°C per century) calculated over the period of 1883 to 1997 based on four different calibration periods for our Sr/Ca data (F14) from Fiji. 95% confidence bounds are shown in parenthesis.

Calibration period	Fiji F14-Sr/Ca
1883-1997	1.19 (0.78 - 1.6)
1960-1997	1.16 (0.76 - 1.57)
1978-1997	0.76 (0.5 - 1.02)
Scaled 1883-1997	0.47 (0.31 - 0.63)

Table S5. Correlation between records from the southwest tropical Pacific. Correlation coefficients between western Pacific coral proxy time series with Fiji composite and F14 Sr/Ca-SST reconstructions (incl. detrended records), the SWCP (Fiji-PHYDA) with trend and detrended and the SWCP based on ERSST5. All correlations between proxy data for full overlap period. All annual mean correlations. Shading and asterisk indicates statistically significant correlations (*light yellow 0.1; **light green 0.05; ***dark green 0.001 significance levels).

	Fiji comp SST	Fiji comp SST (detrended)	F14 SST (detrended)	SWCP (this study)	SWCP (this study detrended)	SWCP ERSSTv5 (detrended)
WP-EIO O2K (*24*)	0.55***	0.58***	0.44***	0.44***	0.52***	0.78***
Fiji Sr/Ca comp.	-0.90***	-0.87***	-0.39***	-0.47***	-0.41***	-0.45***
Fiji $\delta^{18}O$ (*23*)	-	-0.23**	0.12	-0.41***	-0.36***	-0.49***
Vanuatu $\delta^{18}O$ (*81*)	-0.68***	-0.41***	-0.32**	0.55***	-0.59***	-0.45***
Vanuatu $\delta^{18}O$ (*82*)	-0.32**	-0.15	-0.1	-0.40**	-0.27*	-0.23*
Rabaul Sr/Ca (*83*)	0.27*	-0.35***	-0.40***	-0.19*	-0.24**	-0.20*
Rabaul $\delta^{18}O$ (*83*)	-0.44***	-0.30**	-0.28**	-0.17*	-0.17*	-0.22**
New Caledonia Sr/Ca (*16*)	0.39***	0.43***	0.30**	0.39***	0.38***	0.58***
Tonga Sr/Ca (*84*)	-0.57***	-0.47***	-0.37**	-0.35**	-0.29**	-0.375***
Samoa $\delta^{18}O$ (*17*)	-	-0.14*	-0.24**	0.34***	0.13*	0.35***
Rarotonga Sr/Ca (*85*)	0.19	-0.26*	-0.33**	-0.29**	-0.40***	-0.44***
Kavieng Sr/Ca (*86*)	-0.07	-0.15	-0.1	-0.1	-0.1	-0.15
Nauru $\delta^{18}O$ (*87*)	-0.19	0.17	-0.05	0.46**	0.55***	0.52***
Guam $\delta^{18}O$ (*88*)	-0.50***	-0.15	-0.29**	-0.18	-0.1	-0.13
Palau $\delta^{18}O$ (*89*)	-0.59***	-0.35***	-0.33**	-0.42***	-0.40***	-0.51***
Bunaken $\delta^{18}O$ (*88*)	-0.40***	-0.27***	-0.27*	-0.48***	-0.46***	-0.65***

Table S6. Details of the CMIP6 model data used in Fig. 4. Name of the model and number of years of data used from pre-industrial control simulation used to generate the composite maps in figure 4.

S. No.	CMIP6 model	Years
1	BCC-CSM2-MR	600
2	BCC-ESM1	451
3	CAMS-CSM1-0	500
4	CanESM5	1000
5	CMCC-CM2-SR5	500
6	CMCC-ESM2	500
7	CNRM-CM6-1	500
8	CNRM-ESM2-1	500
9	E3SM-1-0	500
10	EC-Earth3	500
11	FGOALS-g3	700
12	GFDL-CM4	500
13	GISS-E2-1-H	800
14	INM-CM4-8	531
15	INM-CM5-0	1200
16	MPI-ESM1-2-HR	500
17	NorCPM1	500
18	NorESM2-LM	500
19	SAM0-UNICON	700
20	UKESM1-0-LL	1880

REFERENCES AND NOTES

1. A. Timmermann, S. I. An, J. S. Kug, F. F. Jin, W. J. Cai, A. Capotondi, K. M. Cobb, M. Lengaigne, M. J. McPhaden, M. F. Stuecker, K. Stein, A. T. Wittenberg, K. S. Yun, T. Bayr, H. C. Chen, Y. Chikamoto, B. Dewitte, D. Dommenget, P. Grothe, E. Guilyardi, Y. G. Ham, M. Hayashi, S. Ineson, D. Kang, S. Kim, W. Kim, J. Y. Lee, T. Li, J. J. Luo, S. McGregor, Y. Planton, S. Power, H. Rashid, H. L. Ren, A. Santoso, K. Takahashi, A. Todd, G. M. Wang, G. J. Wang, R. H. Xie, W. H. Yang, S. W. Yeh, J. Yoon, E. Zeller, X. B. Zhang, El Niño-Southern Oscillation complexity. *Nature* **559**, 535–545 (2018).

2. A. Santoso, M. J. Mcphaden, W. J. Cai, The defining characteristics of ENSO extremes and the strong 2015/2016 El Niño. *Rev. Geophys.* **55**, 1079–1129 (2017).

3. W. J. Cai, L. X. Wu, M. Lengaigne, T. Li, S. McGregor, J. S. Kug, J. Y. Yu, M. F. Stuecker, A. Santoso, X. C. Li, Y. G. Ham, Y. Chikamoto, B. Ng, M. J. McPhaden, Y. Du, D. Dommenget, F. Jia, J. B. Kajtar, N. Keenlyside, X. P. Lin, J. J. Luo, M. Martin-Rey, Y. Ruprich-Robert, G. J. Wang, S. P. Xie, Y. Yang, S. M. Kang, J. Y. Choi, B. L. Gan, G. I. Kim, C. E. Kim, S. Kim, J. H. Kim, P. Chang, Pantropical climate interactions. *Science* **363**, eaav4236 (2019).

4. W. J. Cai, M. Lengaigne, S. Borlace, M. Collins, T. Cowan, M. J. McPhaden, A. Timmermann, S. Power, J. Brown, C. Menkes, A. Ngari, E. M. Vincent, M. J. Widlansky, More extreme swings of the South Pacific convergence zone due to greenhouse warming. *Nature* **488**, 365–369 (2012).

5. W. Q. Han, G. A. Meehl, A. X. Hu, J. Zheng, J. Kenigson, J. Vialard, B. Rajagopalan, Yanto, Decadal variability of the Indian and Pacific Walker cells since the 1960s: Do they covary on decadal time scales? *J. Clim.* **30**, 8447–8468 (2017).

6. H. Heidemann, T. Cowan, S. B. Power, B. J. Henley, Statistical relationships between the Interdecadal Pacific Oscillation and El Niño-Southern Oscillation. *Clim. Dyn.* **188**, 114634 (2023).

7. S. Power, M. Lengaigne, A. Capotondi, M. Khodri, J. Vialard, B. Jebri, E. Guilyardi, S. McGregor, J. S. Kug, M. Newman, M. J. McPhaden, G. Meehl, D. Smith, J. Cole, J. Emile-Geay, D. Vimont, A. T. Wittenberg, M. Collins, G. I. Kim, W. J. Cai, Y. Okumura, C. Chung, K.

M. Cobb, F. Delage, Y. Y. Planton, A. Levine, F. Zhu, J. Sprintall, E. Di Lorenzo, X. B. Zhang, J. J. Luo, X. P. Lin, M. Balmaseda, G. J. Wang, B. J. Henley, Decadal climate variability in the tropical Pacific: Characteristics, causes, predictability, and prospects. *Science* **374**, eaay9165 (2021).

8. J. R. Brown, M. Lengaigne, B. R. Lintner, M. J. Widlansky, K. van der Wiel, C. Dutheil, B. K. Linsley, A. J. Matthews, J. Renwick, South Pacific Convergence Zone dynamics, variability and impacts in a changing climate. *Nat. Rev. Earth Environ.* **1**, 530–543 (2020).

9. R. V. Rohli, G. A. Snedden, E. R. Martin, K. L. DeLong, Impacts of ocean-atmosphere teleconnection patterns on the south-central United States. *Front. Earth Sci.* **10**, 934654 (2022).

10. A. Capotondi, S. McGregor, M. J. McPhaden, S. Cravatte, N. J. Holbrook, Y. Imada, S. C. Sanchez, J. Sprintall, M. F. Stuecker, C. C. Ummenhofer, M. Zeller, R. Farneti, G. Graffino, S. J. Hu, K. B. Karnauskas, Y. Kosaka, F. Kucharski, M. Mayer, B. Qiu, A. Santoso, A. S. Taschetto, F. Wang, X. B. Zhang, R. M. Holmes, J. J. Luo, N. Maher, C. Martinez-Villalobos, G. A. Meehl, R. Naha, N. Schneider, S. Stevenson, A. Sullivan, P. van Rensch, T. T. Xu, Mechanisms of tropical Pacific decadal variability. *Nat. Rev. Earth Environ.* **4**, 754–769 (2023).

11. B. J. Henley, J. Gergis, D. J. Karoly, S. Power, J. Kennedy, C. K. Folland, A tripole index for the interdecadal Pacific oscillation. *Clim. Dyn.* **45**, 3077–3090 (2015).

12. M. H. England, S. McGregor, P. Spence, G. A. Meehl, A. Timmermann, W. J. Cai, A. Sen Gupta, M. J. McPhaden, A. Purich, A. Santoso, Recent intensification of wind-driven circulation in the Pacific and the ongoing warming hiatus. *Nat. Clim. Chang.* **4**, 222–227 (2014).

13. B. K. Linsley, P. P. Zhang, A. Kaplan, S. S. Howe, G. M. Wellington, Interdecadal-decadal climate variability from multicoral oxygen isotope records in the South Pacific Convergence Zone region since 1650 A.D. *Paleoceanography* **23**, 5139 (2008).

14. S. E. Porter, E. Mosley-Thompson, L. G. Thompson, A. B. Wilson, Reconstructing an interdecadal Pacific oscillation index from a Pacific basin-wide collection of ice core records. *J. Clim.* **34**, 3839–3852 (2021).

15. B. M. Buckley, C. C. Ummenhofer, R. D. D'Arrigo, K. G. Hansen, L. H. Truong, C. N. Le, D. K. Stahle, Interdecadal Pacific Oscillation reconstructed from trans-Pacific tree rings: 1350-2004 CE. *Clim. Dyn.* **53**, 3181–3196 (2019).

16. K. L. DeLong, T. M. Quinn, F. W. Taylor, C.-C. Shen, K. Lin, Improving coral-base paleoclimate reconstructions by replicating 350 years of coral Sr/Ca variations. *Palaeogeogr. Palaeoclimatol. Palaeoecol.* **373**, 6–24 (2013).

17. N. Tangri, R. B. Dunbar, B. K. Linsley, D. M. Mucciarone, ENSO's shrinking twentieth-century footprint revealed in a half-millennium coral core from the South Pacific Convergence Zone. *Palaeogeogr. Palaeoclimatol.* **33**, 1136–1150 (2018).

18. B. K. Linsley, H. C. Wu, E. P. Dassié, D. P. Schrag, Decadal changes in South Pacific sea surface temperatures and the relationship to the Pacific decadal oscillation and upper ocean heat content. *Geophys. Res. Lett.* **42**, 2358–2366 (2015).

19. D. M. Thompson, Environmental records from coral skeletons: A decade of novel insights and innovation. *Wiley Interdiscip. Rev. Clim.* **13**, 745 (2022).

20. M. L. Griffiths, A. K. Kimbrough, M. K. Gagan, R. N. Drysdale, J. E. Cole, K. R. Johnson, J. X. Zhao, B. I. Cook, J. C. Hellstrom, W. S. Hantoro, Western Pacific hydroclimate linked to global climate variability over the past two millennia. *Nat. Commun.* **7**, 11719 (2016).

21. N. J. Steiger, J. E. Smerdon, E. R. Cook, B. I. Cook, A reconstruction of global hydroclimate and dynamical variables over the Common Era. *Sci. Data* **5**, 180086 (2018).

22. T. J. Crowley, Causes of climate change over the past 1000 years. *Science* **289**, 270–277 (2000).

23. B. K. Linsley, A. Kaplan, Y. Gouriou, J. Salinger, P. B. deMenocal, G. M. Wellington, S. S. Howe, Tracking the extent of the South Pacific convergence zone since the early 1600s. *Geochem. Geophys. Geosyst.* **7**, 1115 (2006).

24. J. E. Tierney, N. J. Abram, K. J. Anchukaitis, M. N. Evans, C. Giry, K. H. Kilbourne, C. P. Saenger, H. C. Wu, J. Zinke, Tropical sea surface temperatures for the past four centuries reconstructed from coral archives. *Paleoceanography* **30**, 226–252 (2015).

25. A. Newton, R. Thunell, L. Stott, Climate and hydrographic variability in the Indo-Pacific Warm Pool during the last millennium. *Geophys. Res. Lett.* **33**, 27234 (2006).

26. D. W. Oppo, Y. Rosenthal, B. K. Linsley, 2,000-year-long temperature and hydrology reconstructions from the Indo-Pacific warm pool. *Nature* **460**, 1113–1116 (2009).

27. A. C. Clement, R. Seager, M. A. Cane, S. E. Zebiak, An ocean dynamical thermostat. *J. Clim.* **9**, 2190–2196 (1996).

28. R. Seager, M. Cane, N. Henderson, D. E. Lee, R. Abernathey, H. H. Zhang, Strengthening tropical Pacific zonal sea surface temperature gradient consistent with rising greenhouse gases. *Nat. Clim. Chang.* **9**, 517–522 (2019).

29. J. Liu, B. Wang, M. A. Cane, S. Y. Yim, J. Y. Lee, Divergent global precipitation changes induced by natural versus anthropogenic forcing. *Nature* **493**, 656–659 (2013).

30. J. Emile-Geay, K. M. Cobb, M. E. Mann, A. T. Wittenberg, Estimating central equatorial Pacific SST variability over the past millennium. Part I: Methodology and validation. *J. Climate* **26**, 2302–2328 (2013).

31. E. S. Chung, A. Timmermann, B. J. Soden, K. J. Ha, L. Shi, V. O. John, Reconciling opposing walker circulation trends in observations and model projections. *Nat. Clim. Chang.* **9**, 405–412 (2019).

32. R. Seager, N. Henderson, M. Cane, Persistent discrepancies between observed and modeled trends in the tropical Pacific Ocean. *J. Clim.* **35**, 4571–4584 (2022).

33. W. J. Cai, A. Santoso, M. Collins, B. Dewitte, C. Karamperidou, J. S. Kug, M. Lengaigne, M. J. McPhaden, M. F. Stuecker, A. S. Taschetto, A. Timmermann, L. X. Wu, S. W. Yeh, G. J. Wang, B. Ng, F. Jia, Y. Yang, J. Ying, X. T. Zheng, T. Bayr, J. R. Brown, A. Capotondi, K. M. Cobb,

B. L. Gan, T. Geng, Y. G. Ham, F. F. Jin, H. S. Jo, X. C. Li, X. P. Lin, S. McGregor, J. H. Park, K. Stein, K. Yang, L. Zhang, W. X. Zhong, Changing El Niño–Southern Oscillation in a warming climate. *Nat. Rev. Earth Environ.* **2**, 628–644 (2021).

34. S. Lee, M. L'Heureux, A. T. Wittenberg, R. Seager, P. A. O'Gorman, N. C. Johnson, On the future zonal contrasts of equatorial Pacific climate: Perspectives from observations, simulations, and theories. *NPJ Clim. Atmos. Sci.* **5**, 82 (2022).

35. T. D. Damassa, J. E. Cole, H. R. Barnett, T. R. Ault, T. R. McClanahan, Enhanced multidecadal climate variability in the seventeenth century from coral isotope records in the western Indian Ocean. *Paleoceanography* **21**, 1217 (2006).

36. T. Watanabe, A. Juillet-Leclerc, J. P. Cuif, C. Rollion-Bard, Y. Dauphin, S. Reynaud, Recent advances in coral biomineralization with implications for paleo-climatology: A brief overview. *Elsevier Oceanogr. Ser.* **73**, 239–254 (2007).

37. S. Bagnato, B. K. Linsley, S. S. Howe, G. M. Wellington, J. Salinger, Evaluating the use of the massive coral *Diploastrea heliopora* for paleoclimate reconstruction. *Paleoceanography* **19**, 935 (2004).

38. T. Mitsuguchi, T. Uchida, E. Matsumoto, P. J. Isdale, T. Kawana, Variations in Mg/Ca, Na/Ca, and Sr/Ca ratios of coral skeletons with chemical treatments: Implications for carbonate geochemistry. *Geochim. Cosmochim. Acta* **65**, 2865–2874 (2001).

39. S. de Villiers, M. Greaves, H. Elderfield, An intensity ratio calibration method for the accurate determination of Mg/Ca and Sr/Ca of marine carbonates by ICP-AES. *Geochem. Geophys. Geosyst.* **3**, n/a-n/a (2002).

40. J. A. Villaescusa, J. D. Carriquiry, Calibration of Sr/Ca and Mg/Ca paleothermometers in coral Porites sp. from San Benedicto Island, Revillagigedo Archipelago, Mexico. *Cienc. Mar.* **30**, 603–618 (2004).

41. D. Paillard, L. Labeyrie, P. Yiou, Macintosh program performs time-series analysis. *Eos* **77**, 379–379 (1996).

42. T. J. Crowley, T. M. Quinn, F. W. Taylor, C. Henin, P. Joannot, Evidence for a volcanic cooling signal in a 335-year coral record from New Caledonia. *Paleoceanography* **12**, 633–639 (1997).

43. W. H. Quinn, V. T. Neal, "The historical record of El Niño events" in *Climate Since A.D. 1500* (Routledge, 1992).

44. L. Gibert, G. R. Scott, D. Scholz, A. Budsky, C. Ferrandez, F. Ribot, R. A. Martin, M. Leria, Chronology for the Cueva Victoria fossil site (SE Spain): Evidence for early Pleistocene Afro-Iberian dispersals. *J. Hum. Evol.* **90**, 183–197 (2016).

45. Q. C. Yang, D. Scholz, K. P. Jochum, D. L. Hoffmann, B. Stoll, U. Weis, B. Schwager, M. O. Andreae, Lead isotope variability in speleothems—A promising new proxy for hydrological change? First results from a stalagmite from western Germany. *Chem. Geol.* **396**, 143–151 (2015).

46. J. C. Obert, D. Scholz, T. Felis, W. M. Brocas, K. P. Jochum, M. O. Andreae, 230Th/U dating of Last Interglacial brain corals from Bonaire (southern Caribbean) using bulk and theca wall material. *Geochim. Cosmochim. Acta* **178**, 20–40 (2016).

47. H. Cheng, R. L. Edwards, C. C. Shen, V. J. Polyak, Y. Asmerom, J. Woodhead, J. Hellstrom, Y. J. Wang, X. G. Kong, C. Spotl, X. F. Wang, E. C. Alexander, Improvements in ^{230}Th dating, ^{230}Th and ^{234}U half-life values, and U-Th isotopic measurements by multi-collector inductively coupled plasma mass spectrometry. *Earth Planet. Sci. Lett.* **371–372**, 82–91 (2013).

48. B. Y. Huang, P. W. Thorne, V. F. Banzon, T. Boyer, G. Chepurin, J. H. Lawrimore, M. J. Menne, T. M. Smith, R. S. Vose, H. M. Zhang, Extended reconstructed sea surface temperature, version 5 (ERSSTv5): Upgrades, validations, and intercomparisons. *J. Clim.* **30**, 8179–8205 (2017).

49. R. W. Reynolds, N. A. Rayner, T. M. Smith, D. C. Stokes, W. Q. Wang, An improved in situ and satellite SST analysis for climate. *J. Clim.* **15**, 1609–1625 (2002).

50. N. A. Rayner, Global analyses of sea surface temperature, sea ice, and night marine air temperature since the late nineteenth century. *J. Geophys. Res.* **108**, 2670 (2003).

51. A. Kaplan, M. A. Cane, Y. Kushnir, A. C. Clement, M. B. Blumenthal, B. Rajagopalan, Analyses of global sea surface temperature 1856–1991. *J. Geophys. Res.* **103**, 18567–18589 (1998).

52. J. Zinke, A. Hoell, J. M. Lough, M. Feng, A. J. Kuret, H. Clarke, V. Ricca, K. Rankenburg, M. T. McCulloch, Coral record of southeast Indian Ocean marine heatwaves with intensified Western Pacific temperature gradient. *Nat. Commun.* **6**, 8562 (2015).

53. B. L. Otto-Bliesner, E. C. Brady, J. Fasullo, A. Jahn, L. Landrum, S. Stevenson, N. Rosenbloom, A. Mai, G. Strand, Climate variability and change since 850 CE: An ensemble approach with the Community Earth System Model. *Bull. Am. Meteorol. Soc.* **97**, 735–754 (2016).

54. J. H. Jungclaus, K. Lohmann, D. Zanchettin, Enhanced 20th-century heat transfer to the Arctic simulated in the context of climate variations over the last millennium. *Clim. Past* **10**, 2201–2213 (2014).

55. L. Landrum, B. L. Otto-Bliesner, E. R. Wahl, A. Conley, P. J. Lawrence, N. Rosenbloom, H. Y. Teng, Last millennium climate and its variability in CCSM4. *J. Clim.* **26**, 1085–1111 (2013).

56. J. Emile-Geay, K. M. Cobb, M. E. Mann, A. T. Wittenberg, Estimating central equatorial Pacific SST variability over the past millennium. Part II: Reconstructions and implications. *J. Clim.* **26**, 2329–2352 (2013).

57. S. Coats, K. B. Karnauskas, Are simulated and observed twentieth century tropical Pacific sea surface temperature trends significant relative to internal variability? *Geophys. Res. Lett.* **44**, 9928–9937 (2017).

58. I. S. Nurhati, K. M. Cobb, E. Di Lorenzo, Decadal-scale SST and salinity variations in the central tropical Pacific: Signatures of natural and anthropogenic climate change. *J. Clim.* **24**, 3294–3308 (2011).

59. V. Trouet, G. J. Van Oldenborgh, KNMI Climate Explorer: A web-based research tool for high-resolution paleoclimatology. *Tree-Ring Res.* **69**, 3–13 (2013).

60. S. G. Dee, K. M. Cobb, J. Emile-Geay, T. R. Ault, R. L. Edwards, H. Cheng, C. D. Charles, No consistent ENSO response to volcanic forcing over the last millennium. *Science* **367**, 1477–1481 (2020).

61. G. T. Rustic, A. Koutavas, T. M. Marchitto, B. K. Linsley, Dynamical excitation of the tropical Pacific Ocean and ENSO variability by Little Ice Age cooling. *Science* **350**, 1537–1541 (2015).

62. J. L. Conroy, A. Restrepo, J. T. Overpeck, M. Steinitz-Kannan, J. E. Cole, M. B. Bush, P. A. Colinvaux, Unprecedented recent warming of surface temperatures in the eastern tropical Pacific Ocean. *Nat. Geosci.* **2**, 46–50 (2009).

63. C. Torrence, G. P. Compo, A practical guide to wavelet analysis. *Bull. Am. Meteorol. Soc.* **79**, 61–78 (1998).

64. J. M. Lough, Coral calcification from skeletal records revisited. *Mar. Ecol. Prog. Ser.* **373**, 257–264 (2008).

65. T. Mitsuguchi, E. Matsumoto, T. Uchida, Mg/Ca and Sr/Ca ratios of *Porites* coral skeleton: Evaluation of the effect of skeletal growth rate. *Coral Reefs* **22**, 381–388 (2003).

66. S. de Villiers, G. T. Shen, B. K. Nelson, The SrCa-temperature-temperature relationship in coralline aragonite: Influence of variability in $(SrCa)_{seawater}$ and skeletal growth parameters. *Geochim. Cosmochim. Acta* **58**, 197–208 (1994).

67. C. Alibert, M. T. McCulloch, Strontium/calcium ratios in modern *porites* corals from the Great Barrier Reef as a proxy for sea surface temperature: Calibration of the thermometer and monitoring of ENSO. *Paleoceanography* **12**, 345–363 (1997).

68. R. Rashid, A. Eisenhauer, V. Liebetrau, J. Fietzke, F. Bohm, M. Wall, S. Krause, A. Ruggeberg, W. C. Dullo, H. Jurikova, E. Samankassou, B. Lazar, Early diagenetic imprint on temperature proxies in holocene corals: A case study from French Polynesia. *Front. Earth Sci.* **8**, 301 (2020).

69. A. Ribaud-Laurenti, B. Hamelin, L. Montaggioni, D. Cardinal, Diagenesis and its impact on Sr/Ca ratio in Holocene *Acropora* corals. *Int. J. Earth Sci.* **90**, 438–451 (2001).

70. A. Müller, M. K. Gagan, M. T. McCulloch, Early marine diagenesis in corals and geochemical consequences for paleoceanographic reconstructions. *Geophys. Res. Lett.* **28**, 4471–4474 (2001).

71. N. Griffiths, W. Muller, K. G. Johnson, O. A. Aguilera, Evaluation of the effect of diagenetic cements on element/Ca ratios in aragonitic Early Miocene (~16 Ma) Caribbean corals: Implications for 'deep-time' palaeo-environmental reconstructions. *Palaeogeogr. Palaeoclimatol. Palaeoecol.* **369**, 185–200 (2013).

72. E. J. Hendy, M. K. Gagan, J. M. Lough, M. McCulloch, P. B. deMenocal, Impact of skeletal dissolution and secondary aragonite on trace element and isotopic climate proxies in *Porites* corals. *Paleoceanography* **22**, 1462 (2007).

73. N. Allison, A. Finch, J. Webster, D. Clague, Palaeoenvironmental records from fossil corals: The effects of submarine diagenesis on temperature and climate estimates. *Geochim. Cosmochim. Acta* **71**, 4693–4703 (2007).

74. S. de Villiers, B. K. Nelson, A. R. Chivas, Biological controls on coral Sr/Ca and δ18O reconstructions of sea surface temperatures. *Science* **269**, 1247–1249 (1995).

75. R. M. Walter, H. R. Sayani, T. Felis, K. M. Cobb, N. J. Abram, A. K. Arzey, A. R. Atwood, L. D. Brenner, E. P. Dassie, K. L. DeLong, B. Ellis, J. Emile-Geay, M. J. Fischer, N. F. Goodkin, J. A. Hargreaves, K. H. Kilbourne, H. Krawczyk, N. P. McKay, A. L. Moore, S. A. Murty, M. R. Ong, R. D. Ramos, E. V. Reed, D. Samanta, S. C. Sanchez, J. Zinke, The CoralHydro2k Database: A global, actively curated compilation of coral δ18O and Sr/Ca proxy records of tropical ocean hydrology and temperature for the Common Era. *Earth Syst. Sci. Data* **15**, 2081–2116 (2023).

76. J. P. D'Olivo, D. J. Sinclair, K. Rankenburg, M. T. McCulloch, A universal multi-trace element calibration for reconstructing sea surface temperatures from long-lived Porites corals: Removing 'vital-effects'. *Geochim. Cosmochim. Acta* **239**, 109–135 (2018).

77. P. Montagna, M. McCulloch, E. Douville, M. L. Correa, J. Trotter, R. Rodolfo-Metalpa, D. Dissard, C. Ferrier-Pagès, N. Frank, A. Freiwald, S. Goldstein, C. Mazzoli, S. Reynaud, A.

Rüggeberg, S. Russo, M. Taviani, Li/Mg systematics in scleractinian corals: Calibration of the thermometer. *Geochim. Cosmochim. Acta* **132**, 288–310 (2014).

78. T. M. DeCarlo, G. A. Gaetani, A. L. Cohen, G. L. Foster, A. E. Alpert, J. A. Stewart, Coral Sr-U thermometry. *Paleoceanography* **31**, 626–638 (2016).

79. K. M. Cobb, C. D. Charles, H. Cheng, R. L. Edwards, El Niño/Southern Oscillation and tropical Pacific climate during the last millennium. *Nature* **424**, 271–276 (2003).

80. H. R. Sayani, K. M. Cobb, K. DeLong, N. T. Hitt, E. R. M. Druffel, Intercolony δ18O and Sr/Ca variability among *Porites* spp. corals at Palmyra Atoll: Toward more robust coral-based estimates of climate. *Geochem. Geophys. Geosyst.* **20**, 5270–5284 (2019).

81. M. K. Gorman, T. M. Quinn, F. W. Taylor, J. W. Partin, G. Cabioch, J. A. Austin, B. Pelletier, V. Ballu, C. Maes, S. Saustrup, A coral-based reconstruction of sea surface salinity at Sabine Bank, Vanuatu from 1842 to 2007 CE. *Paleoceanography* **27**, PA3226 (2012).

82. T. M. Quinn, T. J. Crowley, F. W. Taylor, New stable isotope results from a 173-year coral from Espiritu Santo, Vanuatu. *Geophys. Res. Lett.* **23**, 3413–3416 (1996).

83. T. M. Quinn, F. W. Taylor, SST artifacts in coral proxy records produced by early marine diagenesis in a modern coral from Rabaul, Papua New Guinea. *Geophys. Res. Lett.* **33**, (2006).

84. H. C. Wu, B. K. Linsley, E. P. Dassié, B. Schiraldi, P. B. deMenocal, Oceanographic variability in the South Pacific Convergence Zone region over the last 210 years from multi-site coral Sr/Ca records. *Geochem. Geophys. Geosyst.* **14**, 1435–1453 (2013).

85. B. K. Linsley, G. M. Wellington, D. P. Schrag, Decadal sea surface temperature variability in the subtropical South Pacific from 1726 to 1997 A.D. *Science* **290**, 1145–1148 (2000).

86. Y. Kawakubo, C. Alibert, Y. Yokoyama, A reconstruction of subtropical western North Pacific SST variability back to 1578, based on a *Porites* Coral Sr/Ca record from the Northern Ryukyus, Japan. *Paleoceanography* **32**, 1352–1370 (2017).

87. T. P. Guilderson, D. P. Schrag, Reliability of coral isotope records from the western Pacific warm pool: A comparison using age-optimized records. *Paleoceanography* **14**, 457–464 (1999).

88. C. D. Charles, K. Cobb, M. D. Moore, R. G. Fairbanks, Monsoon–tropical ocean interaction in a network of coral records spanning the 20th century. *Mar. Geol.* **201**, 207–222 (2003).

89. M. C. Osborne, R. B. Dunbar, D. A. Mucciarone, E. Druffel, J.-A. Sanchez-Cabeza, A 215-yr coral δ18O time series from Palau records dynamics of the West Pacific Warm Pool following the end of the Little Ice Age. *Coral Reefs* **33**, 719–731 (2014).